

---

## On the Urbach rule in SbSI ferroelectric crystal

Studenyyak I.P.<sup>1</sup>, Kranjčec M.<sup>2</sup> and Koperlyos B.M.<sup>1</sup>

<sup>1</sup>Uzhhorod National University, 46 Pidhirna St., 88000 Uzhhorod, Ukraine;  
E-mail: studenyak@dr.com

<sup>2</sup>Geotechnical Department Varaždin, University of Zagreb, 7 Hallerova Aleja,  
42000 Varaždin, Croatia; E-mail: m\_kranjcec@yahoo.com

Received: 30.01.2009

### Abstract

Optical absorption edge of SbSI ferroelectric crystal is studied in a broad temperature range. An Urbach behaviour of the absorption edge is observed in paraelectric ( $T > T_c$ ) and partly in ferroelectric ( $130 \text{ K} < T < T_c$ ) phases, whereas deviations from the Urbach rule are revealed at  $T < 130 \text{ K}$ . The influence of crystal lattice disordering of various types on the Urbach absorption edge parameters is studied. The non-Urbach behaviour of the absorption edge is explained by a presence of dynamic structural disordering due to temperature-dependent phonon-defect interactions.

**Keywords:** phase transition, ferroelectric, absorption edge, Urbach rule

**PACS:** 77.84.-s; 78.40.-q

**UDC:** 535.341

### 1. Introduction

Optical properties of chain quasi-one-dimensional ferroelectric semiconductor SbSI have been extensively studied [1, 2]. The most contradictory issue is explanation of its optical absorption edge behaviour. The data regarding the spectral dependences of optical absorption coefficient in SbSI described by the Urbach rule have been reported for the first time in Ref. [3]. Somewhat later similar results have been obtained for the absorption edge in the temperature range 83–373 K for  $\vec{E} \parallel \vec{c}$  and  $\vec{E} \perp \vec{c}$  polarizations [4, 5] where the Urbach rule has been reported to hold true both for the ferroelectric and paraelectric phases, the edge slope and its shape remaining unchanged in the course of first-order ferroelectric phase transition (PT) at  $T_c = 295 \text{ K}$ . The coordinates of the Urbach bundle convergence point  $E_0$  and  $\alpha_0$  noticeably change at the PT and a step in the temperature dependence of the slope  $\sigma$  of the absorption edge has been observed [6]. However, too high values of the parameter  $\alpha_0$  ( $\alpha_0 \sim 10^9 \text{ cm}^{-1}$ ) derived for the ferroelectric phase for the both  $\vec{E} \parallel \vec{c}$  and  $\vec{E} \perp \vec{c}$  polarizations [6] seem to be doubtful.

Meanwhile, the authors [7] have measured spectral dependences of the absorption coefficient for SbSI in the temperature range 25–298 K and reported that the Urbach rule

is not fulfilled in the ferroelectric range. Instead they have observed a set of "pseudo-Urbach parts" of the absorption edge. In Ref. [8] the absorption edge in the paraelectric phase has also been reported to be described by the Urbach rule, contrary to the ferroelectric phase. Deviations from the Urbach behaviour in the latter have been related to temperature dependence of spontaneous electric polarization and formation of the absorption edge explained in the framework of Sumi-Toyozawa model [9].

Note that Burtsev [10, 11] has elaborated a theory of influence of temperature fluctuations of polarization on the absorption edge shape in ferroelectrics and concluded that for SbSI one should observe an exponential absorption edge in the ferroelectric phase and a near-exponential one in the paraelectric phase. Besides, Burtsev has considered the absorption edge as being determined by a direct zero-phonon allowed electronic transition [10, 11], while the authors [7] have emphasised an important role of indirect electron-phonon transitions.

Thus, in spite of more than 35 years of studies of the nature of optical absorption edge in SbSI ferroelectrics, the results are still contradictory and their explanation seems to be rather complicated. The present paper is aimed at studying the temperature behaviour of the absorption edge in ferroelectric SbSI and explaining it from the point of view of presence of various types of crystal lattice disordering.

## 2. Experimental

SbSI single crystals were grown using a chemical vapour transport method [12]. Spectral dependences of the absorption coefficient  $\alpha$  were studied in the temperature range 25–328 K for the light polarizations  $\vec{E} \parallel \vec{c}$  and  $\vec{E} \perp \vec{c}$ . The measurements of reflectance were performed on specially prepared samples for which reflection from the rear surface could be neglected. Linear absorption coefficient  $\alpha$  as a function of one-surface transmittance,  $T$ , and reflection,  $R$ , was calculated using the well known formula that takes multiple internal reflections into account,

$$\alpha = \frac{1}{d} \ln \left\{ \frac{(1-R)^2}{2T} + \sqrt{\left[ \frac{(1-R)^2}{2T} \right]^2 + R^2} \right\}, \quad (1)$$

where  $d$  denotes the plane-parallel sample thickness. The experimental setup and the corresponding technique had been earlier described in Ref. [13]. The relative error  $\Delta\alpha/\alpha$  in determination of the absorption coefficient did not exceed 10% at  $0.3 \leq \alpha d \leq 3$  [14].

## 3. Results and discussion

### 3.1. Temperature behaviour of absorption edge in SbSI crystal

Since the temperature behaviours of the absorption edge in SbSI crystal are similar for both the  $\vec{E} \parallel \vec{c}$  and  $\vec{E} \perp \vec{c}$  polarizations, we will focus on the analysis for the latter polarization only. The absorption edge spectra of SbSI crystals for the  $\vec{E} \parallel \vec{c}$  polarization

obtained within the temperature interval 25–328 K are shown in Fig. 1. The absorption edge in the paraelectric phase ( $T > T_c$ ) and partly in the ferroelectric phase ( $130 \text{ K} < T < T_c$ ) has an exponential shape (Fig. 1), its temperature behaviour being described by the empirical Urbach rule [15]:

$$\alpha(h\nu, T) = \alpha_0 \exp\left[\frac{\sigma(h\nu - E_0)}{kT}\right] = \alpha_0 \exp\left[\frac{h\nu - E_0}{E_U(T)}\right], \quad (2)$$

where  $E_U$  means the Urbach energy equal to the absorption edge energy width which is inversely proportional to the absorption edge slope ( $E_U^{-1} = \Delta(\ln \alpha) / \Delta(h\nu)$ ),  $\sigma$  is the slope parameter of the absorption edge,  $k$  the Boltzmann constant, and  $\alpha_0$  and  $E_0$  the coordinates of the convergence point of the Urbach absorption edge (see Table 1).

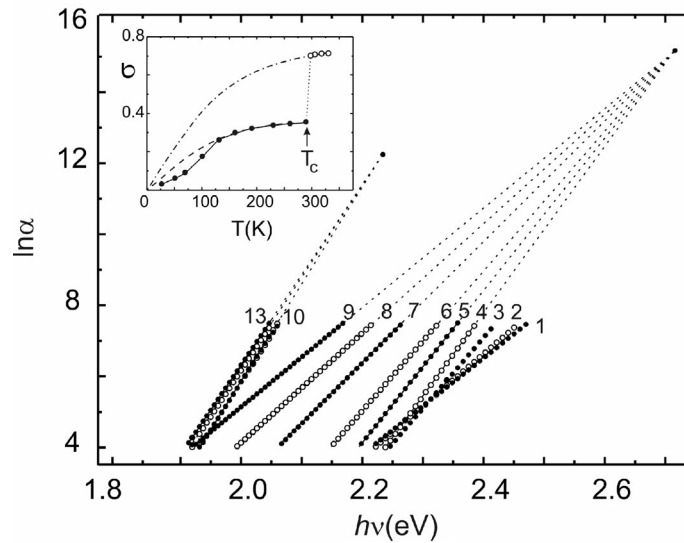


**Fig. 1.** Spectral dependences of absorption coefficient for the SbSI crystal ( $\vec{E} \parallel \vec{c}$  polarization) at different temperatures: 25 K (1), 70 K (2), 100 K (3), 130 K (4), 160 K (5), 190 K (6), 230 K (7), 260 K (8), 290 K (9), 298 K (10), 308 K (11), 318 K (12), 328 K (13). The inset shows temperature dependences of the  $\sigma$  parameter (the experimental data are presented by circles and those calculated according to Eq. (3) – by curves).

The exponential shape and the Urbach behaviour of the long-wavelength absorption edge are usually associated with manifestations of exciton (or electron)–phonon interactions (EPI) [16]. It should be noted that the temperature dependences of the  $\sigma$  parameter for SbSI crystal (see Fig. 1) in the paraelectric phase ( $T > T_c$ ) and partly in the ferroelectric phase ( $130 \text{ K} < T < T_c$ ) are described by the known relation

$$\sigma(T) = \sigma_0 \left( \frac{2kT}{\hbar\omega_p} \right) \tanh\left( \frac{\hbar\omega_p}{2kT} \right), \quad (3)$$

where  $\hbar\omega_p$  denotes the effective phonon energy in frame of single-oscillator model that

describes the EPI and  $\sigma_0$  is the parameter linked with the EPI constant  $g$  through the relation  $\sigma_0 = 2/3g$  [16]. The obtained  $\hbar\omega_p$  and  $\sigma_0$  values are gathered in Table 1. For SbSI crystal we have  $\sigma_0 < 1$ , thus evidencing a strong EPI [17].

Table 1. Urbach absorption edge parameters  $\alpha_0$  and  $E_0$ , EPI parameters  $\hbar\omega_p$  and  $\sigma_0$  and parameters  $\theta_E$ ,  $E_g^*(0)$ ,  $S_g^*$ ,  $(E_U)_0$  and  $(E_U)_1$  of the SbSI crystal for  $\vec{E} \parallel \vec{c}$  polarization obtained after fitting the experimental results with Eqs. (2)–(4) and (6)

Temperature range	$T < T_c$	$T > T_c$
$\alpha_0$ (cm <sup>-1</sup> )	$3.88 \times 10^6$	$2.07 \times 10^5$
$E_0$ (eV)	2.716	2.234
$\hbar\omega_p$ (meV)	27.9	32.1
$\sigma_0$	0.39	0.79
$\theta_E$ (K)	324	372
$E_g^*(0)$ (eV)	2.422	2.126
$(E_U)_0$ (meV)	35.7	20.3
$(E_U)_1$ (meV)	72.5	40.6
$S_g^*$	21.5	6.7

### 3.2. Temperature behaviour of optical pseudogap in SbSI crystal

The temperature dependence of optical pseudogap  $E_g^*$  determined from the absorption edge energy position at a fixed value of optical absorption coefficient ( $\alpha = 10^3$  cm<sup>-1</sup>) is shown in Fig. 2. Temperature variation of  $E_g^*$  due to the EPI can be described using a known relation [18]:

$$E_g^*(T) = E_g^*(0) - S_g^* k \theta_E \left[ \frac{1}{\exp(\theta_E/T) - 1} \right], \quad (4)$$

where  $E_g^*(0)$  is the optical pseudogap at 0 K,  $S_g^*$  a constant number,  $\theta_E$  the Einstein temperature corresponding to the average frequency of phonon excitations for a non-interacting system of harmonic oscillators. The calculations performed by us have evidenced that the experimental values of  $E_g^*$  are well described by Eq. (4) in the paraelectric phase ( $T > T_c$ ) and partly in the ferroelectric phase ( $130 \text{ K} < T < T_c$ ). The  $E_g^*(0)$ ,  $S_g^*$  and  $\theta_E$  parameters obtained for both phases are listed in Table 1, too.

A stepwise variation in the temperature dependence of the optical pseudogap is observed in the PT region (see Fig. 2). Let us now consider the temperature dependence

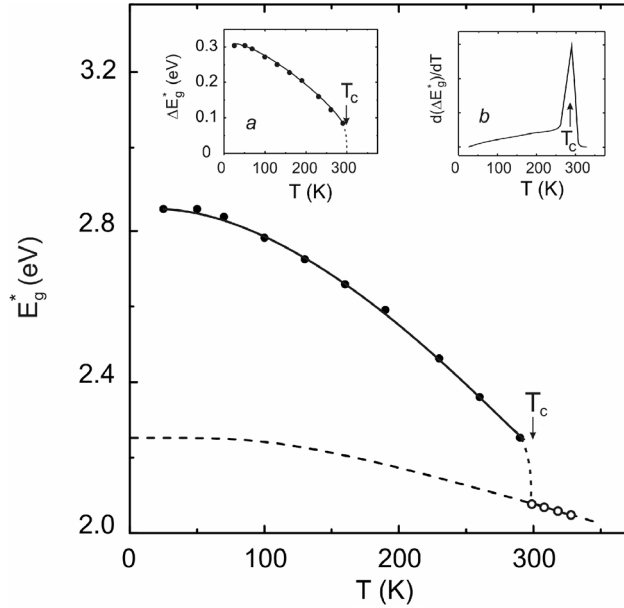


**Fig. 2.** Temperature dependence of optical pseudogap for the SbSI crystal ( $\vec{E} \parallel \vec{c}$  polarization): the experimental data  $E_g^*$  are represented by circles and those calculated from Eq. (4) for the paraelectric phase – by curve. The insets show temperature dependences of  $\Delta E_g^*$  (a) and  $d(\Delta E_g^*)/dT$  (b).

of  $\Delta E_g^*$  variation in the course of PT from the paraelectric to ferroelectric phase in SbSI crystal (see inset (a) in Fig. 2). We have calculated the values of  $\Delta E_g^*(T)$  at  $T < T_c$  as increments of  $E_g^*(T)$  parameter in the ferroelectric phase with respect to that referred to the paraelectric phase:

$$\Delta E_g^*(T) = E_{g,f}^*(T) - E_{g,p}^*(T), \quad (5)$$

where  $E_{g,f}^*(T)$  is the optical pseudogap in the ferroelectric phase and  $E_{g,p}^*(T)$  the values calculated with Eq. (4) on the basis of the corresponding experimental parameters in the paraelectric phase. When calculating  $E_{g,p}^*(T)$  at  $T < T_c$ , we have used the parameters obtained for the paraelectric phase (see Table 1). It is worth noticing that  $\Delta E_g^*(T) = 0$  in the paraelectric phase. The temperature dependence of temperature derivative of the increment  $\Delta E_g^*$  induced by the order parameter is shown in the inset (b) in Fig. 2. It is proportional to anomalous part of specific heat and manifests a maximum at the first-order PT (i.e., near  $T_c$ ).

### 3.3. Temperature-related and structural disordering in SbSI crystal

Temperature dependences of the Urbach energy  $E_U$  (see Fig. 3) in the paraelectric phase ( $T > T_c$ ) and partly in the ferroelectric phase ( $130 \text{ K} < T < T_c$ ) are well described in frame

of the Einstein model by the relation [19]

$$E_U = (E_U)_0 + (E_U)_1 \left[ \frac{1}{\exp(\theta_E/T) - 1} \right], \quad (6)$$

where  $(E_U)_0$  and  $(E_U)_1$  are some parameters constant within the same phase. The  $(E_U)_0$ ,  $(E_U)_1$  and  $\theta_E$  values obtained after fitting the experimental temperature dependence of  $E_U$  (see Fig. 3) with Eq. (6) are shown in Table 1. It should be noted that, similarly to Eq. (4), Eq. (6) has been thoroughly checked for a great number of materials. In recent years it has been most widely used to describe temperature dependences of the optical pseudogap and the Urbach energy [20–22]. The Urbach energy in solids is known to be determined not only by temperature-related disordering, but also by structural one [23]:

$$E_U(T, X) = K \left( \langle u^2 \rangle_T + \langle u^2 \rangle_X \right), \quad (7)$$

where  $K$  is a constant and  $\langle u^2 \rangle_T$  and  $\langle u^2 \rangle_X$  the mean-square deviations (displacements) of atoms from their equilibrium positions due to the temperature-related and structural disordering effects, respectively. Since atomic displacements lead to variations of electric potential of the system, Eq. (7) is then given by

$$E_U = k_0 (W_T^2 + W_X^2) = (E_U)_T + (E_U)_X, \quad (8)$$

where  $k_0$  is a another constant and  $W_T^2$  and  $W_X^2$  the mean-square deviations from the electric potential of a perfect ordered structure, which are driven respectively by the

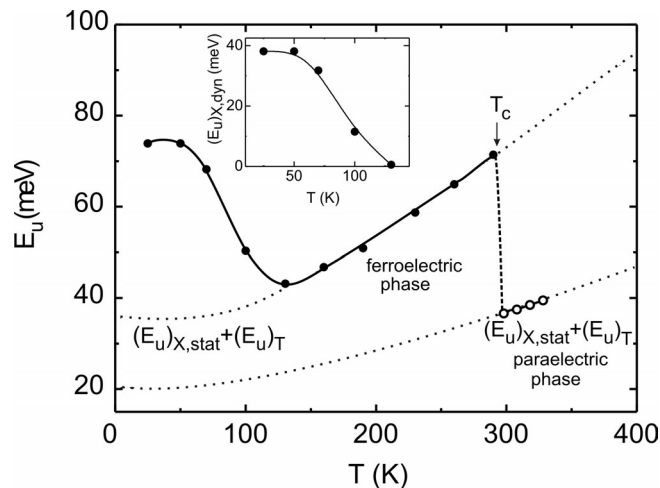


**Fig. 3.** Temperature dependence of Urbach energy for the SbSI crystal ( $\vec{E} \parallel \vec{c}$  polarization): the experimental  $E_U$  values are shown by circles and those calculated from Eq. (6) by curves. The inset shows temperature dependence of dynamic structural disordering contribution  $(E_U)_{X,dyn}$ .

temperature-related and structural disorderings. The contributions of the temperature-related (the term  $(E_U)_T$ ) and the structural ( $(E_U)_X$ ) disorderings to  $E_U$  are considered as being independent, equivalent and additive. The temperature-related disordering occurs owing to thermal vibrations of atoms, thus resulting in smearing of the absorption edge due to EPI.

In order to explain deviations of the optical absorption edge in the ferroelectric phase of SbSI at  $T < 130$  K from the Urbach behaviour and, consequently, an increase in the Urbach energy  $E_U$  with decreasing temperature (see Fig. 3), we present  $(E_U)_X$  as a sum of two components: a static structural disordering ( $(E_U)_{X,stat}$ ) and a dynamic one ( $(E_U)_{X,dyn}$ ). In this case Eq. (8) may be written as

$$E_U = (E_U)_T + (E_U)_{X,stat} + (E_U)_{X,dyn}. \quad (9)$$

One can see that the classification of structural disordering into static and dynamic components is rather nominal, since the dynamic structural disordering could be treated as both structural and temperature-related effects:

$$(E_U)_T = (E_U)_{TV} + (E_U)_{X,dyn}, \quad (10)$$

with  $(E_U)_{TV}$  being the contribution of lattice thermal vibrations. However, in spite of nominal character of the classification noted above, it is the latter that has enabled explaining the anomalous behaviour of the Urbach energy  $E_U$  and the additional disordering occurring at the PT into superionic phase in superionic conductors, as well as in the absence of intermediate order in glassy semiconductors [24–26].

The contribution of temperature-independent static structural disordering  $(E_U)_{X,stat}$  in SbSI crystal originates from a presence of topologically inequivalent arrangements of impurities, differences in the interchain distances and, accordingly, non-uniformity of the interchain van der Waals interactions. The contribution of temperature-dependent dynamic structural disordering  $(E_U)_{X,dyn}$  can be caused by a presence of temperature-dependent phonon-defect interactions due to specific features of van der Waals interchain bonding and impurity arrangement in strongly anisotropic crystals such as SbSI, which have been mentioned in Ref. [12]. The contributions under consideration have been determined using the Einstein temperature  $\theta_E$  and the parameters  $(E_U)_0$  and  $(E_U)_1$  obtained when fitting the temperature dependence of  $E_U$  with Eq. (6).

Hence, the temperature behaviour of the Urbach energy  $E_U$  in the lower-temperature part of the ferroelectric phase (i.e., at  $T < 130$  K) is determined by contributions of all the terms contained in Eq. (9). The  $(E_U)_{X,dyn}$  value decreases and  $(E_U)_T$  increases with increasing temperature, while the  $(E_U)_{X,stat}$  parameter remains constant. A decrease in the Urbach energy  $E_U$  taking place at higher temperatures in the

region of  $T < 130$  K due to decrease in the  $(E_U)_{X,dyn}$  contribution is explained by interaction of some part of defects with phonons, giving rise to an ordering within the defect system. The  $(E_U)_{X,dyn}$  parameter is zero at  $T \geq 130$  K and the temperature behaviour of  $E_U$  is determined by that of  $(E_U)_T$  under the condition of  $(E_U)_{X,stat} = \text{const}$ . After transition from the ferroelectric phase to the paraelectric one both  $(E_U)_{X,stat}$  and  $(E_U)_{X,dyn}$  parameters decrease essentially (see Table 1), causing a stepwise (almost double) decrease in the  $E_U$  value (Fig. 3). An increase of the Urbach energy  $E_U$  occurring inside the paraelectric phase with increasing temperature is associated with increase of the  $(E_U)_T$  value under the condition of constant  $(E_U)_{X,stat}$ .

#### 4. Conclusion

The optical absorption edge of ferroelectric SbSI crystal is studied within the temperature range of 25–328 K. In the paraelectric phase (at the temperatures  $T > T_c$ ) and partly in the ferroelectric phase ( $130 \text{ K} < T < T_c$ ) the absorption edge is shown to correspond to the Urbach rule. A non-Urbach behaviour of the absorption edge at  $T < 130$  K is explained by dynamic structural disordering  $(E_U)_{X,dyn}$ . The latter can be caused by a presence of temperature-dependent phonon-defect interaction, namely the interaction of defects caused by specific features of van der Waals interchain bonding and some features of impurity arrangement in strongly anisotropic SbSI crystals, with thermal vibrations of the lattice involved.

The temperature variations of the optical pseudogap in the paraelectric phase ( $T > T_c$ ) and partly in the ferroelectric one ( $130 \text{ K} < T < T_c$ ) are shown to be well described by the Einstein model. The optical pseudogap reveals stepwise temperature behaviour in the PT vicinity, which is typical for the first-order transitions.

#### References

1. Fridkin V M. Ferroelectrics-semiconductors. Moscow: Nauka (1976).
2. Gerzanich E I and Fridkin V M. Ferroelectrics of  $A^V B^{VI} C^{VII}$  Type. Moscow: Nauka (1982).
3. Kamimura H, Shapiro S M and Balkanski M, 1970. Notes on absorption band edge of SbSI. Phys. Lett. A **33**: 277–278.
4. Zeinally A K, Mamedov A M and Efendiev Sh M, 1973. On absorption edge of SbSI ferroelectric-semiconductor. Fiz. Tekh. Poluprov. **7**: 383–386.
5. Zeinally A K, Mamedov A M and Efendiev Sh M, 1973. A study of SbSI absorption edge. Ferroelectrics **6**: 119–122.
6. Zametin V I and Yakubovskii M A, 1983. Anomalies of SbSI absorption edge. Fiz. Tverd. Tela **25**: 254–257.
7. Borets A N and Kovach D Sh, 1981. Peculiarities of exciton-phonon interaction and



- polarization phenomena on absorption edge of  $A^V B^{VI} C^{VII}$ -type chain semiconductors. *Fiz. Elektronika* **2**: 28–34.
8. Zickus K, Audzjonis A, Batarunas J and Sileika A, 1984. The fundamental absorption edge tail of ferroelectric SbSI. *Phys. Stat. Sol. (b)* **125**: 645–651.
  9. Sumi H and Toyozawa Y, 1971. Urbach-Martienssen rule and exciton trapped momentarily by lattice vibrations. *Techn. Rept.* **452**: 1–53.
  10. Burtsev E V, 1973. On the theory of optical absorption edge spectra of ferroelectric crystals. *Ferroelectrics* **6**: 15–17.
  11. Burtsev E V, 1980. Fluctuation of polarizations and Urbach rule in uniaxial ferroelectrics. *Opt. Spektrosk.* **48**: 80–84.
  12. Bercha D M, Voroshilov Yu V, Slivka V Yu and Turyanitsa I D, Complicate chalcogenides and chalcohalogenides (growth and properties). Lviv: Vyscha Shkola (1983).
  13. Studenyak I P, Kranjcec M, Kovacs Gy S, Panko V V, Desnica I D, Slivka A G and Guranich P P, 1999. The effect of temperature and pressure on the optical absorption edge in  $Cu_6PS_5X$  ( $X = Cl, Br, I$ ) crystals. *J. Phys. Chem. Sol.* **60**: 1897–1904.
  14. Oswald F, 1959. Zur meßgenauigkeit bei der bestimmung der absorptionskonstanten von halbleitern im infraroten spektralbereich. *Optik* **16**: 527–537.
  15. Urbach F, 1953. The long-wavelength edge of photographic sensitivity and electronic absorption of solids. *Phys. Rev.* **92**: 1324–1326.
  16. Kurik M V, 1971. Urbach rule (Review). *Phys. Stat. Sol. (a)* **8**: 9–30.
  17. Sumi H and Sumi A, 1987. The Urbach-Martienssen rule revisited. *J. Phys. Soc. Jap.* **56**: 2211–2220.
  18. Beaudoin M, DeVries A J G, Johnson S R, Laman H and Tiedje T, 1997. Optical absorption edge of semi-insulating GaAs and InP at high temperatures. *Appl. Phys. Lett.* **70**: 3540–3542.
  19. Yang Z, Homewood K P, Finney M S, Harry M A and Reeson K J, 1995. Optical absorption study of ion beam synthesized polycrystalline semiconducting  $FeSi_2$ . *J. Appl. Phys.* **78**: 1958–1963.
  20. Cody G D, 1992. Urbach edge of crystalline and amorphous silicon: a personal review. *J. Non-Cryst. Sol.* **141**: 3–15.
  21. O'Donnell K P and Chen X, 1991. Temperature dependence of semiconductor band gaps. *Appl. Phys. Lett.* **58**: 2924–2926.
  22. Johnson S R and Tiedje T, 1995. Temperature dependence of the Urbach edge in GaAs. *J. Appl. Phys.* **78**: 5609–5613.
  23. Cody G D, Tiedje T, Abeles B, Brooks B and Goldstein Y, 1981. Disorder and the optical-absorption edge of hydrogenated amorphous silicon. *Phys. Rev. Lett.* **47**: 1480–1483.
  24. Studenyak I P, Kranjčec M, Kovacs Gy Sh, Panko V V, Azhnyuk Yu M, Desnica I D, Borets O M and Voroshilov Yu V, 1998. Fundamental optical absorption edge and

- 
- exciton-phonon interaction in  $\text{Cu}_6\text{PS}_5\text{Br}$  superionic ferroelastic. *Mat. Sci. Eng. B* **52**: 202–207.
25. Studenyak I P, Kranjčec M and Kurik M V, 2006. Urbach rule and disordering processes in  $\text{Cu}_6\text{P}(\text{S}_{1-x}\text{Se}_x)_5\text{Br}_{1-y}\text{I}_y$  superionic conductors. *J. Phys. Chem. Sol.* **67**: 807–817.
26. Kranjčec M, Studenyak I P and Kurik M V, 2009. On the Urbach rule in non-crystalline solids. *J. Non-Cryst. Sol.* **355**: 54–57.
- 

***Анотація.** В роботі досліджений оптичний край поглинання сегнетоелектричних кристалів  $\text{SbSI}$  в широкому температурному інтервалі. В параелектричній фазі ( $T > T_c$ ) і частково в сегнетоелектричній фазі ( $130 \text{ K} < T < T_c$ ) спостерігалась урбахівська поведінка краю поглинання, тоді як при  $T < 130 \text{ K}$  виявлене відхилення від правила Урбаха. Досліджений вплив розупорядкування кристалічної ґратки різного типу на параметри урбахівського краю поглинання. Не урбахівська поведінка краю поглинання пояснена динамічним структурним розупорядкуванням викликаним температурно залежною фонон-дефектною взаємодією.*